

Electrosynthesis and solution structure of six-electron reduced forms of metatungstate, $[\text{H}_2\text{W}_{12}\text{O}_{40}]^{6-}$ †

Colette Boskovic,^a Maruse Sadek,^b Robert T. C. Brownlee,^b Alan M. Bond^c and Anthony G. Wedd^{*a}

^a School of Chemistry, University of Melbourne, Parkville, Victoria 3052, Australia.

E-mail: t.wedd@chemistry.unimelb.edu.au; Fax: +61 3 9347 5180

^b Department of Chemistry, La Trobe University, Bundoora, Victoria 3083, Australia

^c Department of Chemistry, Monash University, Clayton, Victoria 3168, Australia

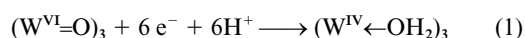
Received 2nd August 2000, Accepted 8th November 2000

First published as an Advance Article on the web 13th December 2000

Metatungstate salts $\alpha\text{-}[\text{R}_4\text{N}]_5\text{H}[\text{H}_2\text{W}_{12}\text{O}_{40}]$ ($\text{R} = \text{Pr}$ or Bu) were produced by phase transfer methods. Two one-electron reduction processes ($E_{1/2} = -1100, -1590$ mV versus Ag-AgCl (saturated KCl in MeCN)) are seen for $[\text{Bu}_4\text{N}]_5\text{H}[\text{H}_2\text{W}_{12}\text{O}_{40}]$ in MeCN (Bu_4NClO_4 , 0.1 M) solution. They convert into a single two-electron process in MeCN–water (95:5 v/v) upon the addition of acid. Controlled potential electrolysis in aqueous HCl at the two electron potentials resulted in isolation of the six-electron reduced salt $[\text{NH}_4]_4\text{H}_8[\text{H}_2\text{W}_{12}\text{O}_{40}]$ in which one of the oxidised W^{VI} trinuclear caps of metatungstate is reduced to a W^{IV} trinuclear cap. $[\text{Bu}_4\text{N}]_3\text{H}_9[\text{H}_2\text{W}_{12}\text{O}_{40}]$ and related salts were generated by phase transfer. The anion $[\text{H}_2\{\text{W}^{\text{IV}}_3(\text{OH})_2\}_3\text{W}^{\text{VI}}_9\text{O}_{34}(\text{OH})_3]^{3-}$ is obtained by dissolving $[\text{Bu}_4\text{N}]_5\text{H}_9[\text{H}_2\text{W}_{12}\text{O}_{40}]$ in dry CD_3CN . The distribution of the eleven protons present in this anion is mapped by ^1H and ^{183}W NMR, allowing assessment of the structural changes which accompany reduction. C_3 point symmetry is observed and imposed by the association of the three surface hydroxyl protons with the reduced W^{IV} trinuclear cap and one of the oxidised W^{VI} trinuclear caps. Three WOW links appear to be converted into longer $\text{W}(\text{OH})\text{W}$ links to accommodate the significant shortening (≈ 0.7 Å) in $\text{W}\cdots\text{W}$ separation anticipated to occur upon reduction.

Introduction

The four trinuclear capping units of Keggin polyoxo anions $[\text{X}^n\text{M}^{\text{VI}}_{12}\text{O}_{40}]^{n-8}$ ($\text{M} = \text{Mo}$ or W ; T_d point symmetry for the α isomer; Fig. 1) are linked to define a tetrahedral cavity encapsulating atom X .^{1a} Reduction produces intensely coloured species, known colloquially as “blues”, in which the added electrons are delocalised over all or part of the molecular framework.^{1b,2,3} However, for the specific cases of $\text{M} = \text{W}$ and for $\text{X}^n = 2\text{H}^+$, B^{III} or Si^{IV} , reduction by exactly six electrons leads to orange-brown anions.^{1b,2} For these “browns” Launay suggested that the total reduction process actually involved the transfer of six electrons and six protons, consistent with localisation of the added electrons in a single trinuclear cap whose terminal oxo ligands are protonated to aqua ligands,² eqn. (1). ^{17}O NMR has detected the oxygen atoms of the aqua



ligands.⁴ The formal presence of three $\text{W}^{\text{IV}}\text{-W}^{\text{IV}}$ bonds⁵ was proposed as the driving force for the electron localisation, consistent with the known structures of trinuclear species of Mo^{IV} and W^{IV} such as $[\text{M}_3\text{O}_4(\text{H}_2\text{O})_9]^{4+}$ and $[\text{Mo}_3\text{O}_4(\text{C}_2\text{O}_4)_3(\text{H}_2\text{O})_3]^{2-}$.⁶⁻⁹

A crystal structure of the 6e^- reduced salt $\text{K}_5\text{H}_6[\text{BW}_{12}\text{O}_{40}]$ confirmed the presence of a W^{IV}_3 cap in the anion and the presence of the α isomer.¹⁰ The mean $\text{W}^{\text{IV}}\text{-W}^{\text{IV}}$ separations are 2.54 Å and are shorter by 0.77 Å than the equivalent intra-cap $\text{W}^{\text{VI}}\cdots\text{W}^{\text{VI}}$ distances. An increase in the terminal WO bond

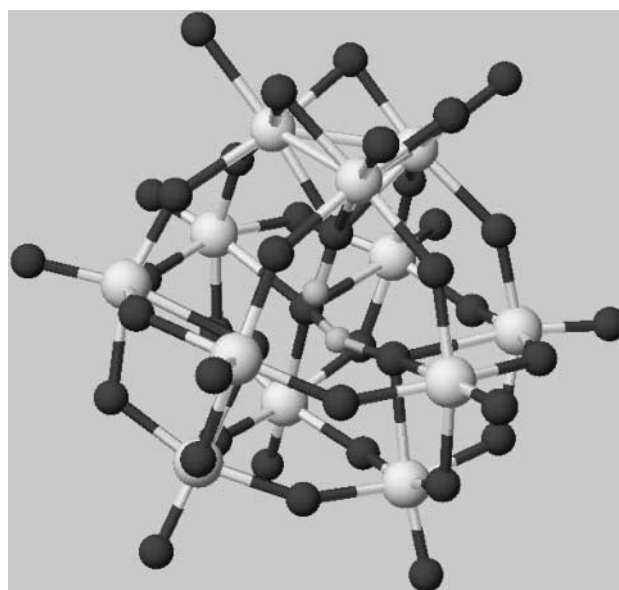


Fig. 1 Ball-and-stick representation of $\alpha\text{-}[\text{X}^n\text{W}^{\text{VI}}_{12}\text{O}_{40}]^{n-8}$ ($\text{X} = 2\text{H}^+$).

length from ≈ 1.7 to ≈ 2.2 Å is consistent with the formation of three terminal aqua ligands in the reduced cap, although the protons were not detected. A disordered crystal structure of the 6e^- reduced metatungstate salt $\text{Rb}_4\text{H}_8[\text{H}_2\text{W}_{12}\text{O}_{40}]$ is also consistent with this interpretation,¹¹ while X-ray photoelectron spectroscopy identified W^{IV} atoms in this system.¹² These structural changes have been confirmed in aqueous solution by ^{183}W NMR experiments.¹³ Three resonances in the ratio 3:3:6 were found, consistent with C_{3v} point symmetry. In addition,

† Electronic supplementary information (ESI) available: cyclic voltammetric and ^1H , ^{17}O , and ^{183}W NMR data for complexes **5** and **6**. See <http://www.rsc.org/suppdata/dt/b0/b006264m/>

one of the resonances occurs in the characteristic tungsten(IV) chemical shift region (δ 1100 to 1600) while the other two are in the tungsten(VI) region (δ –250 to 60).

The gross structural changes that are observed at the 6 e[–] reduced level are suggested to extend to “brown” species at 12 e[–], 18 e[–] and 24 e[–] reduced levels.^{2,4,19} Trinuclear caps of the Keggin structure are proposed to be reduced sequentially. X-Ray photoelectron spectra of the 12 e[–] and 24 e[–] reduced species are consistent with the presence of W^{IV}.¹² However, these highly reduced but poorly soluble species have not been characterised further. More recently, the 6 e[–] reduced “browns” have been used as scaffolds to construct a new class of polyoxo anions.²⁰

The present work reports the synthesis and characterisation of salts of metatungstate in oxidised and 6 e[–] reduced forms. [NH₄]₄H₈[H₂W₁₂O₄₀] and [Bu₄N]₃H₉[H₂W₁₂O₄₀] have been examined in detail. In particular, the anion [H₂{W^{IV}₃(OH)₃}-W^{VI}₉O₃₄(OH)₃]^{3–} is obtained by dissolving the latter in dry CD₃CN. The distribution of the eleven protons present in the anion is mapped by ¹H and ¹⁸³W NMR, allowing assessment of structural changes which accompany reduction. A preliminary report of the structural aspects has appeared.²¹

Experimental

Synthesis and manipulations of reduced solutions were performed in an atmosphere of high purity N₂ using standard Schlenk and syringe techniques. Solids were handled in air but stored under high purity dry dinitrogen. Reagents and solvents were AR or LR grade. For electrochemistry in dry MeCN, HPLC grade solvent was dried over activated Al₂O₃. CD₃CN and (CD₃)₂CO were also dried by stirring over activated Al₂O₃. CD₃OD was distilled from Mg activated with I₂. CD₂Cl₂ was used as received. Prior to use, NMR tubes were rinsed with the dry solvent and dried *in vacuo*. [NH₄]₆[H₂W₁₂O₄₀] **1** was purchased from Aldrich. WO₃ (¹⁸³W, 99 atom%) was purchased from Novachem (Victoria, Australia). Elemental analyses were performed by the Analytische Laboratorien, Elbach, Germany.

Syntheses

Na₄[H₂W₁₂O₄₀] (¹⁸³W, 99 atom%) **2.** WO₃ (99% ¹⁸³W, 1.26 g, 5.45 mmol) was mixed with finely ground Na₂CO₃ (0.607 g, 5.73 mmol) and heated at 630 °C for 2 h. The resulting solid was stirred in water (5 cm³) and insoluble material (0.02 g) removed by centrifugation. The solution was evaporated to dryness and stirred with MeOH (10 cm³). The white solid was isolated by vacuum filtration, washed with MeOH (2 × 10 cm³) and dried at 110 °C for one hour. Yield of Na₂WO₄: 1.38 g, 4.71 mmol, 86%.

A small scale synthesis was adapted from Freedman.²² Na₂WO₄ (1.00 g, 3.41 mmol) was stirred in HCl (6 M, 6 cm³) for 4 h. A finely divided yellow solid was isolated by centrifugation and washed with HCl (0.1 M, 2 × 7 cm³) followed by water (2 × 7 cm³). It was dried in vacuum and heated at 110 °C for 1 hour. Yield of WO₃·H₂O: 0.83 g, 3.3 mmol, 98%. This solid was refluxed with a solution of Na₂WO₄ (99% ¹⁸³W, 0.38 g, 1.3 mmol) in water (25 cm³) for three hours, producing a colourless solution containing a small amount of yellow insoluble material (“phase C”²²). The solid (0.01 g) was removed by centrifugation and the solution evaporated to dryness. The residue was stirred with PrⁱOH (20 cm³), the resulting white solid being isolated by centrifugation and washed with PrⁱOH (2 × 15 cm³). The solid was dried in vacuum. Yield of crude complex **2**: 1.28 g.

[Bu₄N]₅H[H₂W₁₂O₄₀] **3.** To a solution of Bu₄NBr (1.6 g; 5.0 mmol) in CH₂Cl₂ (50 cm³) in a separating funnel was added a solution of complex **1** (2.5 g; 0.83 mmol) in HCl (pH 3;

40 cm³). After vigorous shaking and standing for 1 h two layers were present. The lower layer was collected and the upper aqueous layer extracted with a solution of Bu₄NBr (0.96 g; 3.0 mmol) in CH₂Cl₂ (40 cm³). The lower layer was combined with the first and dried with MgSO₄ overnight. After filtration, the solution was reduced in volume to about 25 cm³. Ethyl acetate was added dropwise with vigorous stirring until incipient precipitation, when the mixture was placed in a freezer. The white crystalline product was isolated by vacuum filtration, washed with CH₂Cl₂–ethyl acetate (1:1) followed by ethyl acetate and dried in air. Yield 2.4 g, 71%. Found: C, 23.28; H, 4.48; N, 1.74; W, 54.05. C₈₀H₁₈₃N₅O₄₀W₁₂ requires C, 23.66; H, 4.54; N, 1.72; W, 54.32%. If a water molecule is included (see text), C₈₀H₁₈₅N₅O₄₁W₁₂ requires C, 23.55; H, 4.57; N, 1.72; W, 54.08%. IR (KBr): (ν WO₄) 944s, (ν W₂O, corner) 879s, (ν W₂O, edge) 784s cm^{–1}. Electronic spectrum (MeCN): λ_{max} 263 nm (ε 4.4 × 10⁴ M^{–1} cm^{–1}). ¹⁸³W NMR (CD₃CN): δ 91.3 (s; W_{1/2} 2.3 Hz). ¹⁷O NMR (CD₃CN): δ 39 (≈4 O; W_{1/2} 820; W₃O); 417 (≈13.5 O; overlapping resonances; W₂O); 433 (≈13.5 O; W_{1/2} 435; W₂O) and 758 (≈11 O; W_{1/2}, 820 Hz; WO₄).

[Pr₄N]₅H[H₂W₁₂O₄₀] **4.** To a solution of (C₆H₁₃)₄NBr (2.4 g; 5.5 mmol) in ethyl acetate (50 cm³) in a separating funnel was added a solution of complex **1** (2.7 g; 0.91 mmol) in HCl (pH 3; 25 cm³). After vigorous shaking and standing for 0.5 h two layers were present. The lower layer was collected and dried with MgSO₄ overnight. After filtration, the solution was stirred vigorously while a solution of Pr₄NBr (1.6 g; 6.0 mmol) in ethyl acetate–CH₂Cl₂ (1/1; 20 cm³) was added dropwise. A white microcrystalline solid was filtered off, washed with PrⁱOH and Et₂O and dried in air. The crude product was recrystallised from MeCN–CH₂Cl₂. Yield 2.2 g, 64%. Found: C, 18.76; H, 3.48; N, 1.82; W, 58.10. C₆₀H₁₄₃N₅O₄₀W₁₂ requires C, 19.06; H, 3.79; N, 1.85; W, 58.35%. If a water molecule is included (see text), C₈₀H₁₈₅N₅O₄₁W₁₂ requires C 18.97; H, 3.85; N, 1.84; W, 58.02%. IR (KBr): (ν WO₄) 942s, (ν W₂O, corner) 878s, 847m, (ν W₂O, edge) 781s cm^{–1}.

[NH₄]₄H₈[H₂W₁₂O₄₀] **5.** A solution of complex **1** (2.0 g, 0.68 mmol) in HCl (0.5 M, 15 cm³) was reduced under N₂ at a mercury pool working electrode at –410 mV *versus* Ag–AgCl (3.5 M KCl) until the passage of 390 C (6e per anion). Cyclic voltammetry indicated no residual [H₂W₁₂O₄₀]^{6–}. The brown solution was transferred aerobically to a Schlenk flask and degassed. All subsequent handling was anaerobic. After standing overnight, the solution was filtered through Celite and reduced in volume to about 2 cm³. MeOH (20 cm³) was added dropwise with rapid stirring. The resulting slurry was filtered, the solid washed with MeOH and dried under vacuum. Yield 1.7 g, 85%. Found: N, 1.93; W, 75.20. H₂₆N₄O₄₀W₁₂ requires N, 1.91; W, 75.34%. IR (KBr): (ν WO₄) 935m, 890sh, (ν W₂O, corner) 838br, (ν W₂O, edge) 731br, 649m cm^{–1}. Electronic spectrum (water): λ_{max} 530 nm, sh (ε 370 M^{–1} cm^{–1}).

[Bu₄N]₃H₉[H₂W₁₂O₄₀] **6.** To a solution of Bu₄NBr (0.93 g, 2.9 mmol) in CH₂Cl₂ (40 cm³) in a separating funnel was added a solution of complex **5** (1.4 g, 0.47 mmol) in HCl (pH 3, 35 cm³). After vigorous shaking, the solution was allowed to stand for two hours to form two layers. The lower layer was collected and the upper aqueous layer extracted with a solution of Bu₄NBr (0.42 g, 1.5 mmol) in CH₂Cl₂ (30 cm³). The lower layer was removed, combined with the first and dried with MgSO₄ overnight. After filtration through Celite, the solution was reduced in volume to about 25 cm³. Ethyl acetate was added dropwise with vigorous stirring to incipient precipitation. Standing at –20 °C provided a brown crystalline product which was filtered off, washed with CH₂Cl₂–ethyl acetate (1:1) and ethyl acetate and dried under vacuum. Yield 1.1 g, 65%. Found: C, 16.04; H, 3.28; N, 1.10; W, 61.30. C₄₈H₁₁₉N₃O₄₀W₁₂ requires C, 16.08;

H, 3.35; N, 1.17; W, 61.55%. IR (KBr): 943m, (ν WO₄) 929m, 871sh, (ν W₂O, corner) 849s, 801m, (ν W₂O, edge) 724s, 652m cm⁻¹. Electronic spectrum (MeCN): λ_{max} 550 nm, sh (ϵ 350 M⁻¹ cm⁻¹).

[Bu₄N]₃H₉[H₂W₁₂O₄₀] (99% ¹⁸³W) 6a. Crude complex **2** (99% ¹⁸³W, 1.28 g) was reduced following the procedure outlined above for the synthesis of **5**. Yield of Na_x[NH₄]_{4-x}H₈[H₂W₁₂O₄₀]: 0.98 g, ≈87%. Conversion into **6a** followed the procedure outlined above for **6**. Yield 0.75 g, 62%. Overall yield based on WO₃, 46%.

[Pr₄N]_{3+x}H_{9-x}[H₂W₁₂O₄₀] 7. A solution of Pr₄NBr (0.21 g, 0.79 mmol) in CH₂Cl₂ (15 cm³) was added dropwise with stirring to complex **6** (0.56 g, 0.16 mmol) in CH₂Cl₂ (25 cm³) producing a brown precipitate. This was recrystallised from MeCN–CH₂Cl₂, washed with CH₂Cl₂ and dried under vacuum. Yield 0.31 g, 57%. Found: C, 14.05; H, 2.92; N, 1.52; W, 63.60%; N/W₁₂, 3.76. The material is formulated as a mixture of [Pr₄N]₃H₉[H₂W₁₂O₄₀] and [Pr₄N]₄H₈[H₂W₁₂O₄₀]. C₃₆H₉₅N₃O₄₀W₁₂ requires C, 12.66; H, 2.80; N, 1.23; W, 64.58. C₄₈H₁₂₂N₄O₄₀W₁₂ requires C, 16.01; H, 3.41; N, 1.56; W, 61.25%. ¹H NMR demonstrated the absence of [Bu₄N]⁺.

[Ph₄As]_{0.5}[Bu₄N]_{2.5}H₉[H₂W₁₂O₄₀] 8. A solution of Ph₄AsCl (0.050 g, 0.12 mmol) in CH₂Cl₂ (5 cm³) was added to a solution of complex **6** (0.42 g, 0.12 mmol) in CH₂Cl₂ (10 cm³). EtOH (30 cm³) was added dropwise with vigorous stirring until incipient precipitation. The solution was allowed to stand at –20 °C. After 5 days, the solid was isolated by filtration, washed with EtOH and dried in vacuum. Yield 0.26 g, 0.071 mmol, 59%. The stoichiometry of this mixed salt was determined from the relative intensities of ¹H NMR resonances characteristic of [Ph₄As]⁺ and [Bu₄N]⁺.

[(C₆H₁₃)₄N]_xH_{12-x}[H₂W₁₂O₄₀] 9. A [(C₆H₁₃)₄N]⁺ salt may be isolated in about 20% yield as an oil by Et₂O precipitation from the lower layer produced by extraction of complex **5** (0.40 g, 0.13 mmol) in HCl (pH 3, 10 cm³) with a solution of (C₆H₁₃)₄NBr (0.25 g, 5.7 mmol) in CH₂Cl₂ (10 cm³).

Instrumental techniques

Electrospray ionisation mass spectra were recorded on a Micromass Quattro II triple quadrupole spectrometer or on a Bruker BioApex 47e Fourier Transform spectrometer fitted with an Analytica electrospray source. Infrared spectra were recorded on a Bio-Rad FTS-165 Fourier Transform spectrometer as pressed KBr discs, electronic spectra on a Hitachi 150–20 spectrophotometer between 200 and 900 nm at a scan rate of 200 nm min⁻¹. pH Measurements were performed *in situ* on degassed solutions using a TPS digital pH meter. This was calibrated with pH 7.00 and 4.00 buffers prior to each use.

Voltammetric measurements were made with a Cypress CS-1090 Electroanalysis System, Version 6.1/2V equipped with a Cypress CYSY-IR potentiostat. Rotating disk electrode (RDE) voltammetry utilised a variable speed Metrohm 628–10 rotator. All voltammetry was performed using a standard three electrode arrangement. This employed a glassy carbon stationary electrode (diameter 3 mm) or rotating disk electrode (diameter 3 mm) as the working electrode and a platinum wire as auxiliary electrode. An aqueous Ag–AgCl (3.5 M KCl) or non-aqueous Ag–AgCl (saturated KCl in MeCN) reference electrode was used for aqueous or MeCN and mixed MeCN–water solutions, respectively. All potentials are quoted relative to these electrodes. For the purposes of calibration, the *E*_{1/2} of a solution of K₃Fe(CN)₆ (1.0 mM in 0.1 M KCl) was measured to be 220 mV relative to the aqueous reference electrode, while that of a solution of Fc (1.0 mM in MeCN with 0.1 M Bu₄N–ClO₄) was measured to be 480 mV relative to the non-aqueous

reference electrode. The error in quoted potentials is estimated to be ±5 mV. Solutions were typically 1.0 mM in analyte with supporting electrolyte as indicated in the text. They were degassed by bubbling nitrogen pre-saturated with the appropriate solvent prior to measurements and a blanket of nitrogen was maintained over the solution at all times. The working electrodes were polished with Al₂O₃ (0.3 mm), rinsed with distilled water and dried in air prior to use. Voltammograms were acquired at room temperature which varied from 19 to 23 °C. Controlled potential electrolysis utilised a BAS PWR-3 potentiostat coupled with an AD Instruments Maclab/2e. The cell consisted of a mercury pool working electrode (diameter 3 cm), a platinum mesh auxiliary electrode and the same Ag–AgCl reference electrode as used for voltammetry. The auxiliary electrode was separated from the electrolysis solution by a salt bridge with a sintered glass plug (porosity 4). Solutions were maintained under a blanket of nitrogen throughout the electrolysis.

Nuclear magnetic resonance

¹H spectra were acquired in 5 mm sample tubes at 399.787 MHz on Varian Unity+400 or Inova400 spectrometers equipped with inverse probes. Typical acquisitions utilised a spectral width of 4000 Hz, 32 to 256 transients of 16 to 32 K data points, and a recycle time of 4 s. Spectra were referenced to sodium 3,3,3-trimethyl-1-propane sulfonate at δ 0.00 for D₂O solutions or residual protonated solvent at δ (MeCN) 1.95, δ (CH₂Cl₂) 5.32, δ (Me₂CO) 2.05 and δ (MeOD) 3.35. COSY, TOCSY, NOESY and ROESY (rotating-frame Overhauser enhancement spectroscopy) experiments were acquired at 25 °C using a 90° pulse of 4.1 μ s. Spectra were collected over a spectral width of 4000 Hz, with 128 to 256 increments of 2 K data points, 12 or 16 transients per increment and a recycle time of 4 s. Spectral analysis utilised zero filling to 2 K data points in the first dimension to obtain a symmetrical matrix of 2 K × 2 K data points and a 50 to 80° shifted sine bell window was applied in each dimension. Magnitude COSY 90 experiments were employed. TOCSY, NOESY and ROESY experiments were acquired in phase sensitive mode using the simultaneous hypercomplex method.²³ TOCSY experiments employed an MLEV-16 spin lock flanked by 2 ms trim pulses with a decoupler power resulting in 30 μ s pulses. ROESY experiments utilised an effective spin locking field of 5 kHz with flip angle pulses of 30°. Mixing times of 40 to 80 (TOCSY), 100 to 400 (NOESY) and 50 to 200 ms (ROESY) were employed. ¹⁸³W spectra were acquired in 10 mm sample tubes on a Bruker DRX500 spectrometer equipped with a broadband probe at 30 °C. The reference was an external replacement sample of Na₂WO₄ (2 M in D₂O). Spectra were acquired at 20.837 MHz using a 60° pulse of 26 μ s. Typical acquisitions utilised a spectral width of 4000 Hz, 100 to 10 000 transients of 16 to 32 K data points and a recycle time of 2 to 4 s. A pre-acquisition delay of 100 to 150 ms was used to remove rolling baseline effects caused by pulse breakthrough. Spectra were processed with a line broadening of 1 Hz. COSY 90 spectra were acquired using a 90° pulse of 39 μ s. Experiments over the tungsten-(vi) and -(iv) chemical shift regions were acquired separately due to their large separation. Spectra were collected over a spectral width of 3531 or 1766 Hz, with 64 to 128 increments of 1 or 2 K data points, 1024 or 2048 transients per increment and a recycle time of 1.5 to 2.5 s. Spectral analysis utilised zero filling to 2 K data points in the first dimension to obtain a symmetrical matrix of 2 K × 2 K data points and an unshifted sine bell window was applied in each dimension. Gradient non-phase sensitive ¹H–¹⁸³W HMQC (heteronuclear multiple quantum correlation) experiments were acquired in 5 mm sample tubes on a Bruker DRX400 spectrometer equipped with an inverse probe at 25 °C. The probe was tuned to 400.130 MHz for ¹H and 16.671 MHz for ¹⁸³W. 90° pulses were typically 15.3 μ s for ¹H and 44 ms for

Table 1 ^1H NMR data (400 MHz) for α -metatungstate salts at 22 °C

Compound	Conditions (conc./M, solvent)	Anion protons δ [$W_{1/2}$ /Hz, intensity]	Cation protons	
			δ [multiplicity, intensity, ^a assignment]	Theoretical intensity ^b
Oxidized anions				
1	0.05, D ₂ O	6.01 [1.9, 2.0]	7.10 [s, 24, NH ₄ ⁺ ; $W_{1/2}$, 74 Hz]	
3	0.05, CD ₃ CN	6.80 [0.7, 2.0]	0.98 [t, 55, CH ₃ CH ₂ CH ₂ CH ₂ N]	60
			1.43 [m, 35, CH ₃ CH ₂ CH ₂ CH ₂ N]	40
			1.66 [m, 36, CH ₃ CH ₂ CH ₂ CH ₂ N]	40
			3.20 [m, 39, CH ₃ CH ₂ CH ₂ CH ₂ N]	40
6 e [−] Reduced anions				
Rb ₄ H ₈ [H ₂ W ₁₂ O ₄₀] ^c	D ₂ O	7.2		
5	0.2, D ₂ O	7.18 [3.9, 2.0 H _e]	6.94 [1 : 1 : 1 t, NH ₃ D ⁺ ; ² J _{HD} 52 Hz]	
6	0.15, CD ₃ CN	7.11 [8.6, 2.1 H _a]	0.98 [t, 33, CH ₃ CH ₂ CH ₂ CH ₂ N]	36
		7.22 [2.4, 2.0 H _d]	1.43 [m, 25, CH ₃ CH ₂ CH ₂ CH ₂ N]	24
		7.61 [2.5, 1.0 H _c]	1.65 [m, 26, CH ₃ CH ₂ CH ₂ CH ₂ N]	24
		8.55 [7.3, 2.0 H _b]	3.19 [m, 27, CH ₃ CH ₂ CH ₂ CH ₂ N]	24
		8.76 [7.7, 3.9 H _a]		

^a Estimated assuming 2 protons present on the anion; the order of magnitude difference in the number of anion and cation protons renders these estimates approximate. ^b Assumes five and three cations per anion for complexes **3** and **6**, respectively. ^c Ref. 37.

^a Estimated assuming 2 protons present on the anion; the order of magnitude difference in the number of anion and cation protons renders these estimates approximate. ^b Assumes five and three cations per anion for complexes **3** and **6**, respectively. ^c Ref. 37.

^{183}W . Spectra were collected over spectral widths of 1653 or 4223 Hz for ^1H and 5000 Hz for ^{183}W , with 64 to 256 increments of 4 K data points, 16 to 256 transients per increment and a recycle time of 1.5 to 3.5 s. Spectral analysis utilised zero filling to 1 K data points in the first dimension to obtain a matrix of 4 K \times 1 K data points. The mixing times used are described in the Discussion section. ^{17}O spectra were acquired in 10 mm sample tubes on a Varian Unity+400 spectrometer equipped with a broadband probe at 50 °C without sample spinning, at 54.196 MHz using a 90° pulse of 10 μs . Typical acquisitions utilised a spectral width of 80 000 Hz, 70 000 to 150 000 transients of 8 to 16 K data points and a recycle time of 0.05 to 0.1 s. Spectra were processed with 15 Hz line broadening and displayed with baseline correction.

Results and discussion

Metatungstate salts

Attempts to produce quaternary ammonium salts of $[\text{H}_2\text{W}_{12}\text{O}_{40}]^{6-}$ by direct precipitation from aqueous solution gave materials whose solubility behaviour suggested the presence of mixed cation species. However, salts $[\text{R}_4\text{N}]_5\text{H}[\text{H}_2\text{W}_{12}\text{O}_{40}]$ ($\text{R} = \text{Bu}$; **3** or Pr **4**) produced by phase transfer methods^{24,25} demonstrated a useful range of solubilities in organic solvents. Elemental analyses and relative intensities of ^1H NMR resonances for cation and cavity H_2W_{12} protons of the anion (Table 1) indicate that these salts contain only five R_4N^+ cations per metatungstate ion. Potentiometric titration with base confirmed the presence of an extra proton, although it could not be observed in dry solvent by ^1H NMR. This suggests the presence of lattice H_3O^+ or H_5O_2^+ cations²⁶ rather than an hydroxo ligand.^{27,29} ESI-MS (cone voltage, 20 V) of MeCN solutions of **3** displayed peaks at m/z 1787, 1666 and 1545 whose line separations allow assignment to ion clusters $\{[\text{Bu}_4\text{N}^+]_{4-x}\text{H}^+[\text{H}_2\text{W}_{12}\text{O}_{40}]^{6-}\}^{2-}$ ($x = 1-3$). Presumably, the protons in these gaseous clusters are present as hydroxo ligands to the cluster. In addition, solvated ion clusters $\{[\text{Bu}_4\text{N}^+]_5-x\text{H}^+_{x-}[\text{H}_2\text{W}_{12}\text{O}_{40}]^{6-} \cdot y\text{MeCN}\}^-$ ($x = 2-4$; $y = 0-2$) are observed in the range $m/z = 3095-3660$. At the higher cone voltage of 60 V fragmentation occurs with the entire series $[\text{W}_x\text{O}_{3x+1}]^{2-}$ ($x = 3-12$) being observed. These are formed sequentially by loss of neutral WO_3 . Lower members of this series ($x = 3-7$) have been observed previously from fragmentation of $[\text{W}_6\text{O}_{19}]^{2-}$ and $[\text{W}_{10}\text{O}_{32}]^{4-}$ under CID (collision-induced dissociation) conditions.³⁰

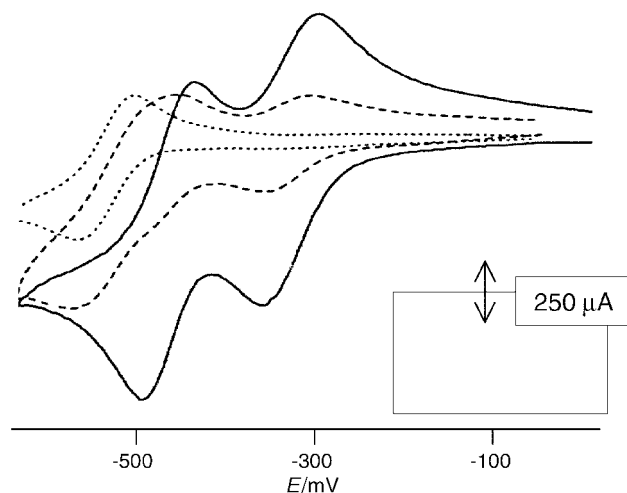


Fig. 2 Cyclic voltammetric monitoring of the electrolysis at -410 mV of complex **1** (0.1 M) in HCl (0.5 M). $v = 100$ mV s^{−1}. — initial; ---- semi-reduced; fully reduced. The differing current intensities reflect the different diffusion coefficients for the oxidised and 6 e[−] reduced species.³⁵

While the ^1H NMR spectrum of $[\text{H}_2\text{W}_{12}\text{O}_{40}]^{6-}$ in aqueous solution has been reported,^{2,31,32} the new data in MeCN and acetone (Tables 1 and ESI S2) indicate that the chemical shift of the cavity H_2W_{12} protons is characteristic of each solvent and essentially independent of the cation. The number of ^{183}W and ^{17}O resonances (see Experimental section) exhibited by complex **3** in CD₃CN is consistent with the effective T_d point symmetry of the α isomer (Fig. 1) in solution and equivalent to that seen in D₂O.^{32,33}

Metatungstate exhibits two chemically reversible 1 e[−] reduction processes in basic aqueous solution at pH 8 which convert into a single 2 e[−] process upon addition of acid.^{15,17,31} The complex coupled electron and proton transfer processes involved, including estimation of reduction potentials and protonation constants, have been examined recently *via* simulation of cyclic voltammetry.³⁴ A second 2 e[−] process is present at pH < 2 (Fig. 2). Two 1 e[−] reduction processes ($E_{1/2} - 1100, -1590$ mV *versus* Ag–AgCl (saturated KCl in MeCN)) are seen also for **3** in MeCN (1.0 mM; Bu₄NClO₄, 0.1M) solution. Medium effects cause these to shift to -920 and -1150 mV in MeCN–water (95:5 v/v). They convert into a single 2 e[−] process upon

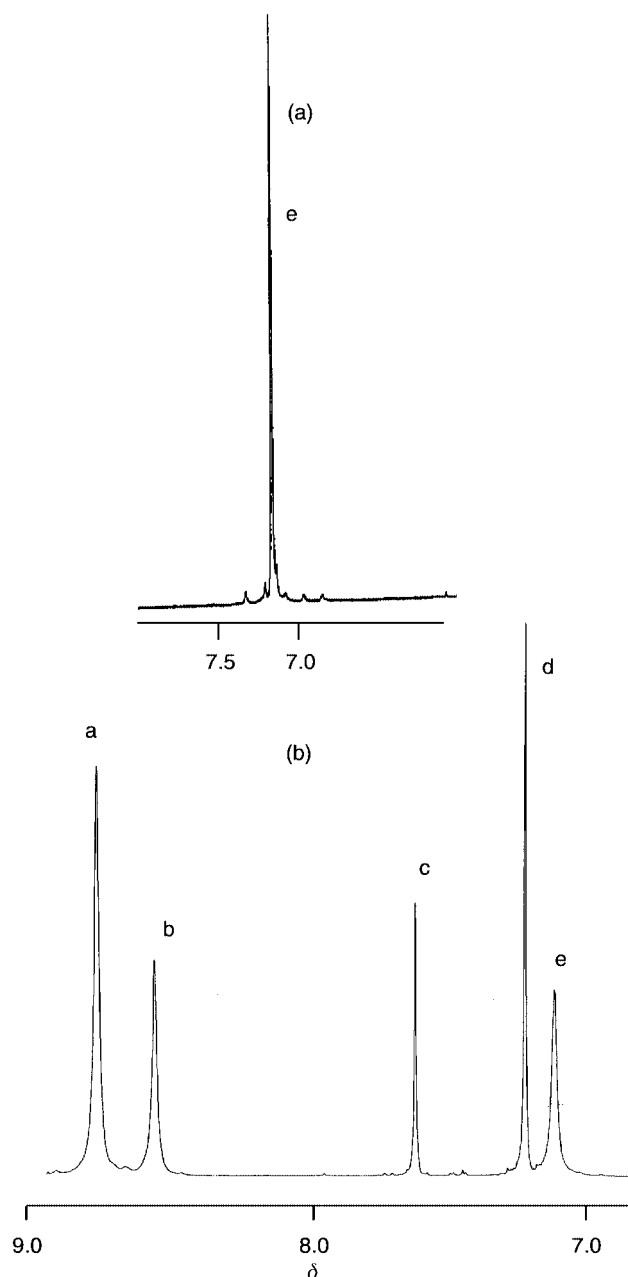


Fig. 3 ^1H NMR spectra (400 MHz) of (a) complex **5** (0.2 M) in D_2O , (b) **6** (0.15 M) in CD_3CN .

addition of HClO_4 (5 mM) and a second 2e^- process is also observed.³⁵

Six-electron reduced salts

Reduction to this level follows electrolysis of metatungstate (0.1 M) in aqueous HCl (0.5 M) at a potential more negative than the first 2e^- process (-320 mV versus $\text{Ag}-\text{AgCl}$ (3.5 M KCl); Fig. 2).^{2,17} The product may disproportionate to the 6e^- level or, more likely, Nernstian shifts in potentials induced by protonation permit direct reduction to the 6e^- level on the timescale of the electrolysis.³⁶ However, the 6e^- reduced species is reduced further at -510 mV which results in precipitation of a 12e^- reduced hydrous oxide.^{2,17} An optimal electrolysis potential of -410 mV in the present work resulted in solutions containing essentially pure 6e^- reduced product (Fig. 2).

This procedure led to pure $[\text{NH}_4]_4\text{H}_8[\text{H}_2\text{W}_{12}\text{O}_{40}]$ **5** via precipitation with MeOH . Organo-soluble $[\text{Bu}_4\text{N}]_3\text{H}_9[\text{H}_2\text{W}_{12}\text{O}_{40}]$ **6** was obtained by extraction of the ammonium salt into CH_2Cl_2 with Bu_4NBr . Other quaternary salts (**7–9**) may also be isolated (see Experimental section). ESI-MS of all reduced

products was similar to those of the analogous oxidised salts. Apparently, the electrospray ionisation process leads to oxidation.

The electrochemistry of complex **5** in aqueous solution follows that described generally for 6e^- reduced solutions.^{16,17} In particular, both cyclic and RDE voltammograms in HCl (0.5 M) reveal an oxidative process (whose limiting current i_L is consistent with a 6e^- oxidation), a chemically reversible 2e^- reductive process (best described as two unresolved 1e^- processes) and a multielectron irreversible process (ESI Fig. S1).³⁵ On the other hand, **6** displays no reductive processes in MeCN in the potential range 0 to -2000 mV versus $\text{Ag}-\text{AgCl}$. However, in $\text{MeCN}-\text{water}$ (95:5 v/v) **6** becomes electroactive in the presence of acid (ESI Fig. S2). Two chemically reversible reductive 2e^- processes are present after the addition of 20 equivalents of HClO_4 (ESI Table S1). In fact, the behaviour is very similar to that of the oxidised salt **3** under these conditions (*cf.* Fig. 2).

The ^1H NMR spectrum of complex **5** in D_2O displays a singlet at $\delta 7.18$, in good agreement with the literature value for the rubidium salt (Table 1; Fig. 3).³⁷ This resonance H_e is assigned to the two internal protons and is shifted 1.2 ppm to higher frequency relative to the oxidised form. At sufficiently high concentration, several weak resonances ($\delta 7.15$, 7.23 , 7.37) may be observed close to the base of the major peak. As their relative intensities increase in heated or aged samples they may be due to different isomers or protonation states. In addition, a low intensity 1:1:1 triplet at $\delta 6.94$ ($J 52\text{ Hz}$) is present in the D_2O solution (Fig. 3). It is also present in DCl solutions of NH_4Cl or of the oxidised salt **1** but not in their D_2O solutions. It is assigned to NH_3D^+ , indicating that the surface protons on the 6e^- reduced metatungstate anion exchange with those of NH_4^+ .

In dry solvents five resonances H_a-H_e are observed for complex **6** in the $\delta 7-9$ range (Fig. 3; Table 1). Peak H_e (intensity 2) at $\delta 7.11$ may be assigned to the internal protons as it is also present in wet solvents. Resonances H_a-H_d (intensities 4:2:1:2) integrate for a total of nine protons and are assigned to those bound to the surface of the anion, observable because of the relatively slow rate of exchange in dry solvent. The detection of these eleven protons confirms the empirical stoichiometry $\text{6} \equiv [\text{Bu}_4\text{N}]_3\text{H}_9[\text{H}_2\text{W}_{12}\text{O}_{40}]$ deduced from microanalysis. Six of them can be assumed to originate from the terminal aqua ligands on the reduced cap, while the other three are most probably located on doubly bridging oxygen atoms as hydroxo ligands. It was apparent that the effective point group of the anion was lower than the C_{3v} symmetry observed in aqueous solution.¹³ Surface protons have been directly detected by ^1H NMR for $[\text{Bu}_4\text{N}]_3\text{H}_3[\text{V}_{10}\text{O}_{28}]$ in CD_3CN ($\delta 9.3$, 6.6).³⁸

Resonance H_e due to the internal protons of complex **6** was also observed in CD_2Cl_2 , $(\text{CD}_3)_2\text{CO}$ and CD_3OD (ESI Table S2). Observation of surface protons varied with the solvent. Very similar peak patterns were observed in CD_3CN and CD_2Cl_2 solutions which were sufficiently dry for the free water peak to be absent. Only three peaks of low relative intensity were apparent at $\delta \approx 9.7$ in $(\text{CD}_3)_2\text{CO}$ and none at all in CD_3OD . The apparent water content of these solvents was 3 and 1 equivalent per anion in the respective solvents. Essentially identical spectra for four different salts of 6e^- reduced metatungstate (**6–9**) were observed in the $\delta 7-9$ range in CD_3CN (ESI Table S3), indicating that ion clustering is not a determinant of the effective point symmetry.

The ^{183}W NMR spectrum of complex **5** in D_2O is in good agreement with the literature (Fig. 4; Table 2).¹³ Three resonances are present in the ratio 3:3:6, consistent with effective C_{3v} point symmetry. The resonance at $\delta 1362.2$ may be assigned to W^{IV} .¹³ In contrast, for **6** in CD_3CN , the three resonances are replaced by seven in the ratio 1:2:2:2:2:2:1 (Fig. 4; Table 2). Resonances W_A and W_B , integrating for 1 and 2 atoms respectively, are assigned to W^{IV} . The combined ^1H and

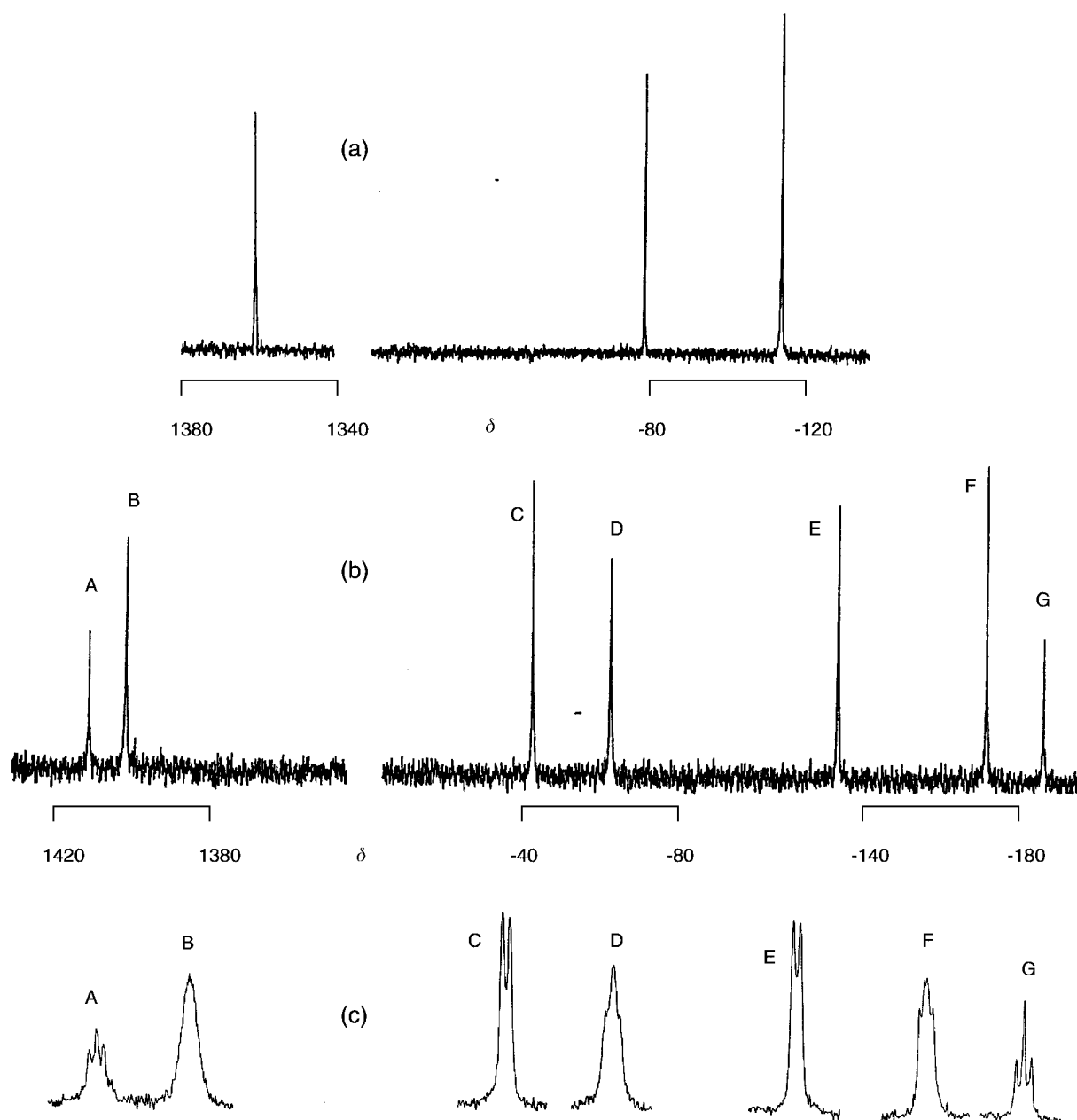


Fig. 4 ^{183}W NMR spectra (20.84 MHz) of (a) complex **5** (0.2 M) in D_2O , (b) **6** (0.15 M) in CD_3CN , (c) **6a** (99% ^{183}W ; 0.1 M; 30 °C) in CD_3CN ; 29696 transients.

^{183}W NMR data are consistent with a reduction in effective point symmetry from C_{3v} for **5** in D_2O to C_s for **6** in CD_3CN . This must be induced by localisation of protons on the surface of the anion, with exchange being slow on both NMR time-scales. Resonances are broader in CD_3CN than in D_2O (Tables 1 and 2), consistent with slow exchange. ^1H – ^{183}W coupling cannot be resolved in either medium.

A ^{17}O NMR spectrum was obtained for complex **5** in D_2O (ESI Fig. S3; Table 2)³⁹ but could not be resolved for **6** in CD_3CN , presumably due to the lower effective symmetry (twentyfive oxygen environments) combined with a lower solubility. For **5** seven resonances are resolved for the eleven oxygen environments anticipated for C_{3v} point symmetry. Five peaks occur in the region expected for the total of 24 doubly bridging oxygen atoms (total observed relative intensity, 21.5) and two in the region for the 9 terminal oxygen atoms (11.4). In contrast to the oxidised anion (see Experimental section), resonances could not be observed for the 4 triply bridging oxygen atoms which define the central cavity occupied by the two internal protons.

Structure of the six-electron reduced anion in solution

The initial NMR data indicated that proton exchange rates are reduced significantly in dry CD_3CN , allowing NMR detection of surface-bound protons and differentiation of inequivalent tungsten sites. Samples of complexes **5** and **6** were enriched to 82–99 atom% ^{183}W to allow detection of WOW coupling and application of 2-D NMR techniques to probe the significant structural changes which accompany reduction.

^1H – ^{183}W HMQC spectra were acquired for complex **5** (82 atom% ^{183}W) in D_2O (Fig. 5). J_{HW} coupling is not apparent in the one dimensional ^1H spectrum but must be less than the linewidth (≈ 4 Hz). Mixing times t_m of 60 and 250 ms were employed to detect coupling in the range 1–10 Hz ($t_m = 1/2J$). Connectivities were detected between the two internal protons and the three W^{IV} atoms in the reduced cap and the six W^{VI} atoms in the belt. A model of C_s point symmetry is presented in Fig. 6: tungsten atoms AB_2 define the reduced cap while atoms $\text{D}_2\text{E}_2\text{F}_2$ define the belt. No connectivity to the three W^{VI} atoms in the corner-shared triad C_2G was evident. This

Table 2 ^{183}W (20.84 MHz) and ^{17}O (54.20 MHz) NMR data for 6e^- reduced metatungstate salts

Nucleus	Salt (conc./M; solvent)	Resonance	δ	$W_{1/2}/\text{Hz}$	Relative intensity	Multiplicity ^a
^{183}W	6e^- reduced solution ^b (0.5; DCl)		1355.4	1.6	3	
			−82.0	1.6	3	
			−115.0	2.9	6	
	5 (0.12; D_2O)		1362.2	2.2	3	
			−77.2	2.2	3	
			−114.8	4.1	6	
	6 (0.15; CD_3CN)	W_A	1413.2	4.4	1	
		W_B	1402.7	5.7	2	
		W_C	−42.6	5.7	2	
		W_D	−64.5	7.1	2	
		W_E	−128.7	4.5	2	
		W_F	−171.0	3.4	2	
		W_G	−187.4	5.2	1	
	6 99% ^{183}W (0.10; CD_3CN)	W_A	1416.5	41.8	1.1	t (15.8)
		W_B	1406.6	40.6	2.0	m
		W_C	−41.9	29.5	2.0	d (16.0)
		W_D	−64.4	41.8	2.1	m
		W_E	−128.9	27.8	2.0	d (14.9)
		W_F	−169.1	35.1	1.9	d of d (12.3, 17.7)
		W_G	−188.1	35.6	0.9	t (17.5)
^{17}O	5 (0.12; D_2O)		727	898	11.4 ^c	
			705	380	^c	
			528	121	3.3	
			461	285	5.0	
			426	440	4.0	
			309	568	7.9	
			237	35	1.3	

^a Overall width of multiplet, Hz. ^b Ref. 13; cation not specified. ^c Combined intensity.

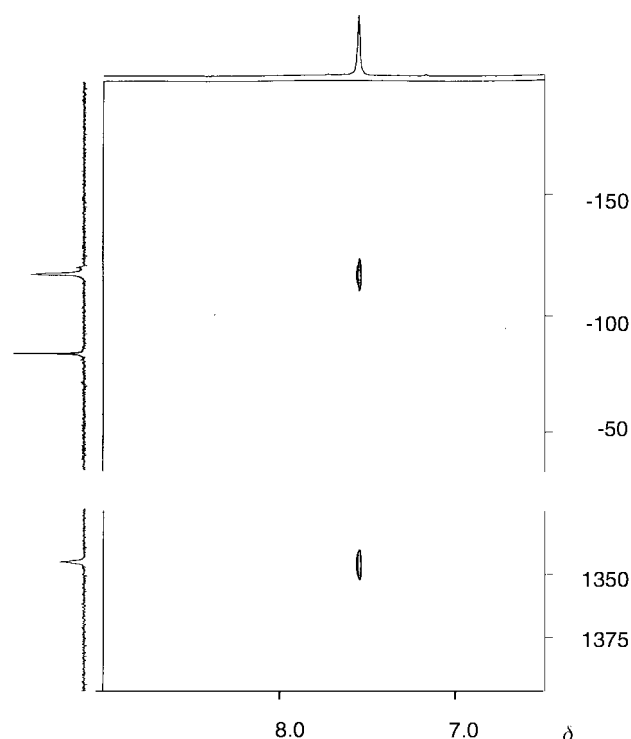


Fig. 5 ^1H – ^{183}W HMQC spectrum of complex **5** (82% ^{183}W , 0.05 M in D_2O ; t_m 60 ms; 25 °C; 64×4 K, 16 transients per increment). ^1H NMR was acquired at 400 MHz.

observation is consistent with localisation of the protons e close to the reduced cap. It supports the suggestion, derived from the detection of fine structure on the tungsten(IV) resonance following deuteration of e, that these protons bind preferentially to the triply bridging $\text{W}^{\text{IV}}_3\text{O}$ oxygen atom, effectively forming an internal aqua ligand $\text{W}^{\text{IV}}_3(\text{OH}_2)$.¹³ The coupling observed to the tungsten(VI) belt resonances must then be interpreted as $^4J_{\text{HOWOW}}$ scalar coupling.

^1H and ^{183}W 1-D NMR spectra for complex **6** in dry CD_3CN

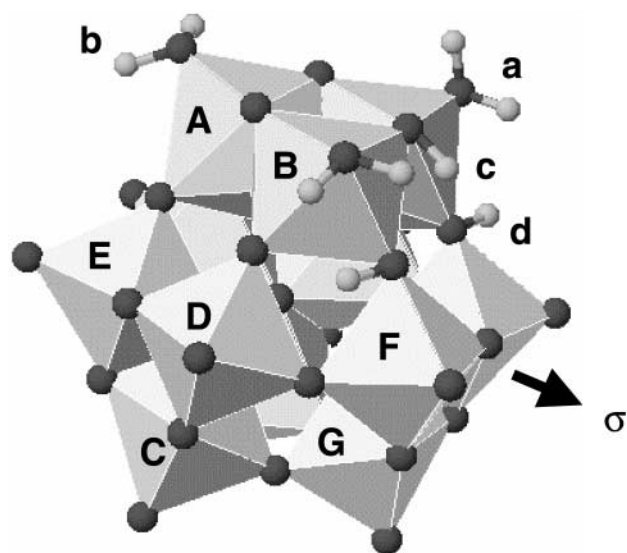


Fig. 6 Polyhedral representation of $[\text{H}_2\{\text{W}^{\text{IV}}_3(\text{OH}_2)_3\}\text{W}^{\text{VI}}_9\text{O}_{34}(\text{OH})_3]^{3-}$ as present in solutions of complex **6** in dry CD_3CN . W atoms are centred in each “octahedron” of O atoms.

indicate C_s point symmetry for the anion (Figs. 3, 4). Resonances W_A and W_G of intensity 1 must be assigned to the unique W^{IV} and W^{VI} atoms lying on the mirror plane (Fig. 6). Then resonance W_B of intensity 2 can be assigned to the pair of W^{IV} atoms related by the plane and the four resonances W_C – W_F of intensity 2 to the remaining four pairs of W^{VI} atoms.

Water addition experiments indicated that the different proton environments display different exchange rates (Fig. 7; ESI Table S4). The five resonances H_a – H_e broaden in the order $H_c > H_d > H_a \approx H_b \gg H_e$. This behaviour allowed H_e to be assigned to the internal protons e. The similar chemical shifts (Fig. 3), exchange rates (Fig. 7) and relative intensities (4:2) allow assignment of H_a and H_b to the $\text{W}^{\text{IV}}(\text{OH}_2)$ ligand protons. Consequently, the fragments $W_A\text{O}(\text{H}_b)_2$ and $\{\text{W}_B\text{O}(\text{H}_a)_2\}_2$ are identified (Fig. 6).

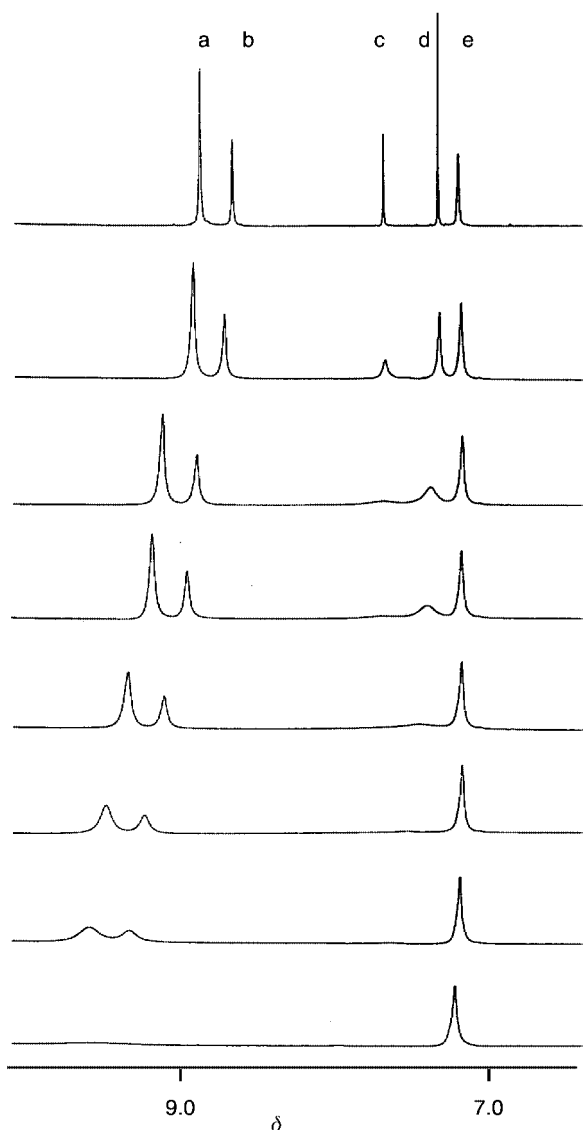


Fig. 7 ^1H NMR spectra (400 MHz) of complex **6** in CD_3CN (0.05 M; 25 °C; 64 transients). Added water (equivalents): 0.5, 1.5, 7, 9, 14, 20, 30, 100 from top to bottom.

The seven separate resonances W_A – W_G are shifted but not broadened by addition of 100 equivalents of water (ESI Table S5). The two tungsten(IV) resonances W_A and W_B display the largest shifts ($\Delta\delta$ +12.2, +24.1), consistent with the presence of terminal aqua ligands rendering them most sensitive to H_2O exchange. The tungsten(VI) resonances W_F (+6.2) and W_G (+1.9) also shift to higher frequency while W_C , W_D and W_E each shift to lower frequency (–4.0 to –6.3). However, relatively small changes in chemical shifts of ^{183}W resonances upon water addition are difficult to interpret.³¹

The ^{183}W NMR spectrum of **6a**, *i.e.* **6** enriched to 99 atom% ^{183}W featured resolved fine structure (13–18 Hz; Table 2; Fig. 4c) assigned as $^2J_{\text{WOW}}$ scalar coupling characteristic of corner-sharing WOW bridges.⁴⁰ The smaller coupling characteristic of edge-sharing links was not resolved.¹³ The situation may be complicated by the effects of longer range coupling.

The assigned resonances W_A and W_G are triplets consistent with each being corner-shared to two equivalent W atoms (Fig. 6). On the other hand, W_C and W_E are clearly doublets, indicating that their pairs of W atoms are corner-shared with unique W atoms A or G. W_F is clearly resolved as a doublet of doublets, which W_D also appears to be, although the resolution is poorer here. Each of their W atoms must be corner coupled to two inequivalent W.

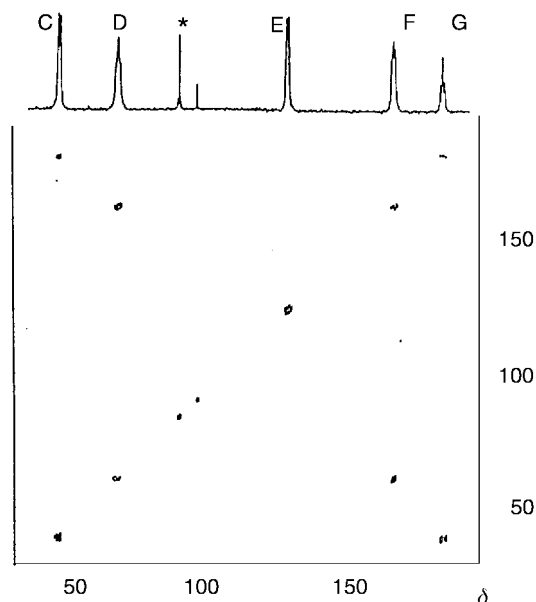


Fig. 8 ^{183}W COSY spectra (20.84 MHz) of complex **6** (99% ^{183}W ; 0.1 M in CD_3CN ; 30 °C). Low frequency region ($64 \times 1\text{K}$, 1024 transients per increment).

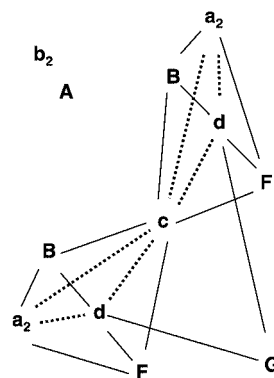


Fig. 9 Map of dipolar HH (-----) and scalar WH (—) connectivities of resonances H_a – H_d of complex **6**. Longer range interactions $\text{H}_\text{b}\text{H}_\text{d}$ and $\text{W}_\text{A}\text{H}_\text{d}$ are also observed but omitted for clarity.

^{183}W COSY experiments proved to be problematical in dry CD_3CN , even for **6a** enriched to 99 atom% ^{183}W . Lower solubility, probe insensitivity, relatively faster relaxation of tungsten(IV) nuclei compared to W^VI and the large chemical shift differences between these centres are the probable causes. However, important results were achieved in the low frequency tungsten(VI) region (Fig. 8). Two crosspeaks are observed: $\text{W}_\text{C}\text{W}_\text{G}$ and $\text{W}_\text{D}\text{W}_\text{F}$. The former allows assignment of, first, W_C to the pair of tungsten atoms C corner-sharing to unique atom G and, secondly, W_E to the pair of tungsten atoms E corner-sharing with unique atom A (Fig. 6). Crosspeak $\text{W}_\text{D}\text{W}_\text{F}$ suggests the assignment given in Fig. 6, given that atoms D and F are each corner-shared to atoms B (see above). However, the data are also consistent with positions D and F being switched.

The location of the three protons c and d determines the point symmetry and their assignment was addressed initially by a series of H–H correlation experiments. Magnitude COSY and TOCSY experiments failed to detect scalar coupling between the different proton environments. Cross peaks $\text{H}_\text{a}\text{H}_\text{c}$, $\text{H}_\text{a}\text{H}_\text{d}$, $\text{H}_\text{b}\text{H}_\text{d}$ and $\text{H}_\text{c}\text{H}_\text{d}$ were observed in NOESY and ROESY experiments (ESI Fig. S4). These dipolar interactions are mapped in Fig. 9. No interactions were observed between internal protons e and any of the external protons a–d.

Mapping of WH scalar interactions utilised HMQC experiments. ^{183}W – ^1H coupling was not detected in the 1-D spectra

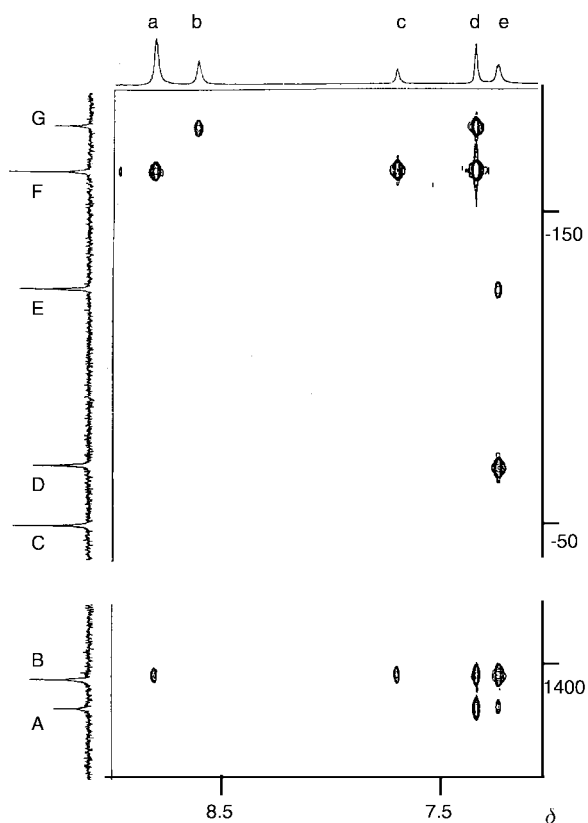


Fig. 10 ^{183}W - ^1H HMQC spectrum of complex **6** (0.15 M) in CD_3CN (t_m 60 ms; 128×4 K, 256 transients per increment; 25°C). ^1H NMR was acquired at 400 MHz.

(cf. Figs. 1, 2) implying that $^2J_{\text{WOH}} < W_{1/2} = 2\text{--}9$ Hz, allowing constraints to be set on mixing times t_m . A spectrum is shown in Fig. 10 and the derived scalar connectivities are included in Fig. 9. This first application of HMQC experiments for locating external protons on polyoxometalates brings some problems of interpretation. Some connectivities may not be detected and some of the observed crosspeaks may involve magnetisation transfer through coupled spin systems. This is certainly possible given the extensive H-H dipolar coupling observed (see Fig. 9). The multiple connectivities displayed by resonances H_c and H_d may involve such magnetisation transfer. In addition, the effect of ^1H exchange on the results of the experiment is unknown.

However, a number of conclusions can be drawn from the present data (Fig. 10). (1) The assignments of W_D and W_F are strengthened by the absence of a connectivity W_DH_d and the presence of connectivities W_FH_d and W_GH_d . (2) The two internal protons e are coupled to the W^{IV} cap AB_2 and to four of the tungsten(vi) belt atoms, D_2 and E_2 . Coupling to the other W^{VI} atoms (C, F and G) is not detected. This is consistent with localisation of the internal protons close to the reduced cap, as deduced previously¹³ and in the present work for complex **5**. (3) The three external protons c and d are coupled to two of the caps only, the reduced cap AB_2 and the unique oxidised cap GF_2 . The external and internal protons appear to avoid each other. The conclusion is consistent with the observed H-H dipolar connectivities, which indicate that all of the external protons are relatively close together on the surface of the anion (Fig. 9).

The mapping indicates that hydrogen atoms c and d may be assigned to three hydroxyl protons associated with the reduced $\text{W}^{\text{IV}}_3(\text{AB}_2)$ and unique $\text{W}^{\text{VI}}_3(\text{GF}_2)$ caps (Figs. 6, 9). This imposes the observed point symmetry of the anion. Another possibility is for unique atom c to be localised as $\text{H}_d\text{--O--H}_c\text{--O--H}_d$, i.e. as a fragment H_3O_2^- . Such hydrated hydroxide ions have been observed in crystals⁴¹ and also as ligands bridging pairs of metal atoms.^{42,43} In the latter cases the reported OHO

linkages are generally close to linear and the $\text{O}\cdots\text{O}$ distances are smaller than the relevant distances observed in $6e^-$ reduced $[\text{H}_2\text{W}_{12}\text{O}_{40}]^{6-}$ and $[\text{BW}_{12}\text{O}_{40}]^{5-}$ (2.4–2.5 versus 3.0–3.1 Å).^{10,11} Consequently, an hydrated hydroxyl ligand is unlikely to be a feature of the present system. Nevertheless, the structure may well involve multiple interactions and exchange between the three hydroxyl hydrogen atoms c and d and the four bridging oxygen atoms in the vicinity and between the four aqua ligand hydrogen atoms a. This may be the source of the significant NMR linewidths observed even in dry solvents (Table 1).

The NMR data are consistent with either an α - or a β -Keggin structure in which the reduced cap is rotated by 60° .^{1a} Distinction between the two isomers requires detection of the ^{183}W - ^{183}W crosspeaks between the tungsten-(iv) and -(vi) resonances. However, the presence of the α isomer in the crystal structures of $6e^-$ reduced $\text{Rb}_4\text{H}_8[\text{H}_2\text{W}_{12}\text{O}_{40}]$ and $\text{K}_5\text{H}_6[\text{BW}_{12}\text{O}_{40}]$ ^{10,11} and the relative instability of β isomers suggest that the α structure is likely for $6e^-$ reduced metatungstate in solution.

Two intriguing aspects connected with proton exchange and magnetisation transfer phenomena can be discerned in the present data. (1) A crosspeak W_GH_b is seen in some HMQC experiments (e.g. Fig. 10) suggesting a connection between atoms on opposite sides of the molecule. Proton exchange may play a role in detection of crosspeaks in HMQC experiments (evolution time 60–100 ms), i.e. some WH crosspeaks (W_GH_b , W_FH_a) may be modulated by HH exchange. (2) WH connectivities in W--OH_2 fragments do not appear consistently. W_AH_b crosspeaks have not been observed by HMQC experiments and W_BH_a crosspeaks are seen in some experiments only (e.g. see Fig. 10). This may be in part due to the effect of relatively faster relaxation rates for tungsten(iv) nuclei.

Conclusion

The isolation of soluble salts of $6e^-$ metatungstate reduced ions is reported. The structures of complex **5** $\equiv [\text{NH}_4]_4\text{H}_8\text{--}[\text{H}_2\text{W}_{12}\text{O}_{40}]$ and **6** $\equiv [\text{Bu}_4\text{N}]_3\text{H}_9\text{--}[\text{H}_2\text{W}_{12}\text{O}_{40}]$ have been examined in solution. The anion present in dry CD_3CN solutions of **6** can be formulated as $[\text{H}_2\{\text{W}^{\text{IV}}_3(\text{OH}_2)_3\}\text{W}^{\text{VI}}_9\text{O}_{34}(\text{OH})_3]^{3-}$ (Fig. 6). The observed C_s point symmetry is imposed by the positions of the three hydroxyl protons c and d. The electronic feature which drives this localisation of protons is the localisation of the six added electrons in the reduced cap AB_2 . In six-electron reduced $\text{K}_5[\text{B}^{\text{III}}\{\text{W}^{\text{IV}}_3(\text{OH}_2)_3\}\text{W}^{\text{VI}}_9\text{O}_{37}]\cdot 13.5\text{H}_2\text{O}$, the $\text{W}^{\text{IV}}\text{--W}^{\text{IV}}$ bond lengths (mean 2.543(3) Å) in the reduced cap are ≈ 0.77 Å shorter than the $\text{W}^{\text{VI}}\cdots\text{W}^{\text{VI}}$ separations in the oxidised caps.¹⁰ The resulting mismatch in dimensions causes the boron atom to move ≈ 0.4 Å within the internal BO_4 unit and away from the reduced cap but C_{3v} symmetry is retained. The internal cavity in metatungstate derivatives features two hydrogen atoms only and the $6e^-$ reduced anion accommodates the mismatch in a different way: three WOW links are converted into longer $\text{W}(\text{OH})\text{W}$ links (Fig. 6).

Acknowledgements

A. G. W. and A. M. B. thank the Australian Research Council for support via Grants A29531579 and A294801726.

References

- M. T. Pope, *Heteropoly and Isopoly Oxometalates*, Springer-Verlag, Berlin, 1983, (a) pp. 23–27; (b) pp. 101–106.
- J. P. Launay, *J. Inorg. Nucl. Chem.*, 1976, **38**, 807.
- M. Sadakane and E. Steckhan, *Chem. Rev.*, 1998, **98**, 219.
- K. Pieprgrass and M. T. Pope, *J. Am. Chem. Soc.*, 1989, **111**, 753.
- F. A. Cotton, *Inorg. Chem.*, 1964, **3**, 1217.
- R. K. Murmann and S. E. Shelton, *J. Am. Chem. Soc.*, 1980, **102**, 3984.

- 7 E. O. Schlemper, M. S. Hussian and R. K. Murmann, *Cryst. Struct. Commun.*, 1982, **11**, 89.
- 8 M. Segawa and Y. Sasaki, *J. Am. Chem. Soc.*, 1985, **107**, 5565.
- 9 A. Bino, F. A. Cotton and Z. Dori, *J. Am. Chem. Soc.*, 1978, **100**, 5252.
- 10 T. Yamase and E. Ishikawa, *J. Chem. Soc., Dalton Trans.*, 1996, 1619.
- 11 Y. Jeannin, J. P. Launay and M. A. Seid Sedjadi, *Inorg. Chem.*, 1980, **19**, 2933.
- 12 L. P. Kazansky and J. P. Launay, *Chem. Phys. Lett.*, 1977, **51**, 242.
- 13 K. Piepgrass and M. T. Pope, *J. Am. Chem. Soc.*, 1987, **109**, 1586.
- 14 C. Tourné, *Bull. Soc. Chim. Fr.*, 1967, 3196; C. Tourné, *Bull. Soc. Chim. Fr.*, 1967, 3199; C. Tourné, *Bull. Soc. Chim. Fr.*, 1967, 3214.
- 15 P. Souchay and J. P. Launay, *C. R. Acad. Sci., Ser. C*, 1969, **268**, 1354.
- 16 J. P. Launay, *C. R. Acad. Sci., Ser. C*, 1969, **269**, 971.
- 17 J. P. Launay, P. Souchay and M. Boyer, *Collect. Czech. Chem. Commun.*, 1971, **36**, 741.
- 18 G. Hervé, *Ann. Chim.*, 1971, **6**, 219; G. Hervé, *Ann. Chim.*, 1971, **6**, 287.
- 19 J. M. Fruchart and G. Hervé, *Ann. Chim.*, 1971, **6**, 337.
- 20 M. H. Dickman, T. Ozeki, H. T. Evans, Jr., C. Rong, G. B. Jameson and M. T. Pope, *J. Chem. Soc., Dalton Trans.*, 2000, 149.
- 21 C. Boskovic, M. Sadek, R. T. C. Brownlee, A. M. Bond and A. G. Wedd, *Chem. Commun.*, 1999, 533.
- 22 M. L. Freedman, *J. Am. Chem. Soc.*, 1959, **81**, 3834.
- 23 A. A. Bothner-By, R. L. Stephens, J. M. Lee, C. D. Warren and R. W. Jeanloz, *J. Am. Chem. Soc.*, 1984, **106**, 811.
- 24 F. Corigliano and S. Di Pasquale, *Inorg. Chim. Acta*, 1975, **12**, 99.
- 25 D. E. Katsoulis and M. T. Pope, *J. Am. Chem. Soc.*, 1984, **106**, 2737.
- 26 G. M. Brown, M. R. Noe-Spirlet, W. R. Busing and H. A. Levy, *Acta Crystallogr., Sect. B*, 1977, **33**, 1038.
- 27 M. V. Capparelli, D. M. L. Goodgame, P. B. Hayman and A. C. Skapski, *J. Chem. Soc., Chem. Commun.*, 1986, 776.
- 28 V. W. Day, W. G. Klemperer and D. J. Maltbie, *J. Am. Chem. Soc.*, 1987, **109**, 2991.
- 29 M. I. Khan, J. Zubietta and P. Toscano, *Inorg. Chim. Acta*, 1992, **193**, 17.
- 30 T. C. Lau and J. Wang, *J. Chem. Soc., Chem. Commun.*, 1995, 877.
- 31 M. T. Pope and G. M. Varga, Jr., *Chem. Commun.*, 1966, 653.
- 32 J. J. Hastings and O. W. Howarth, *J. Chem. Soc., Dalton Trans.*, 1992, 209.
- 33 K. Piepgrass, J. N. Barrows and M. T. Pope, *J. Chem. Soc., Chem. Commun.*, 1989, 10.
- 34 P. D. Prenzler, C. Boskovic, A. M. Bond and A. G. Wedd, *Anal. Chem.*, 1999, **71**, 3650.
- 35 C. Boskovic, PhD thesis, University of Melbourne, 1998.
- 36 P. J. S. Richardt, R. W. Gable, A. M. Bond and A. G. Wedd, *Inorg. Chem.*, in press.
- 37 J. P. Launay, M. Boyer and F. Chaveau, *J. Inorg. Nucl. Chem.*, 1976, **38**, 243.
- 38 V. W. Day, W. G. Klemperer and D. J. Maltbie, *J. Am. Chem. Soc.*, 1987, **109**, 2991.
- 39 A spectrum of a 6e reduced metatungstate species has been described briefly (see ref. 4).
- 40 J. Lefebvre, F. Chauveau, P. Doppelt and C. Brevard, *J. Am. Chem. Soc.*, 1981, **103**, 4589.
- 41 M. Schmidt, A. Schier, J. Riede and H. Schmidbauer, *Inorg. Chem.*, 1998, **37**, 3452 and refs. therein.
- 42 M. Ardon and A. Bino, *Struct. Bonding (Berlin)*, 1987, **65**, 1.
- 43 M. Ardon, A. Bino and K. Michelson, *J. Am. Chem. Soc.*, 1987, **109**, 1986.